

Conclusion

A number of results can be summarized here. By employing deuterated ion precursors we are able to prepare selectively CH_2CCH^- or CH_3CC^- . An ion beam of the former is photodetached by 488-nm laser light, while a beam of the latter species is not. Examination of the photoelectron spectra of CH_2CCH^- , CD_2CCH^- , and CH_2CCD^- allows us to deduce the structures of the ions. On the basis of present evidence for the structure of the propargyl radical, $\text{CH}_2\text{C}\equiv\text{CH}$, and isotope effects observed in our spectra, we conclude that the detaching species is $\text{CH}_2=\text{C}=\text{CH}^-$ and not $^-\text{CH}_2\text{C}\equiv\text{CH}$. The vibration excited in the resulting $\text{CH}_2\text{C}\equiv\text{CH}$ resulting from detachment is a harmonic mode (510 cm^{-1}) and is most likely the $\text{C}\equiv\text{C}-\text{H}$ out-of-plane deformation. The electron affinities of several isotopically substituted propargyl radicals are collected together in Table III. Gas-phase acidities of $\text{CH}_2=\text{C}=\text{CH}_2$ and $\text{CH}_3\text{C}\equiv\text{CH}$ are computed. We are unable to detach $\text{CH}_3\text{C}\equiv\text{C}^-$ and conclude that $\text{EA}(\text{CH}_3\text{C}\equiv\text{C}^-) > 2.60\text{ eV}$. On the basis of this and a conjecture

for the $\Delta H^\circ_{\text{acid}}(\text{H}-\text{CCCH}_3)$, we conclude that $\Delta H^\circ(\text{H}-\text{CCCH}_3) > 125\text{ kcal/mol}$.

Acknowledgment. We thank H. Benton Ellis, Jr., for his assistance and constant advice in operating the photoelectron spectrometer. Suzanne Paulson and Prof. Gary A. Molander assisted us in the synthesis and purification of methylacetylene- d_1 . We would like to acknowledge Prof. John Bartmess for a helpful discussion of the gas-phase acidity of methylacetylene. Financial support for this work was provided by the Research Corp., the donors of the Petroleum Research Foundation, administered by the American Chemical Society, and the United States Department of Energy (Contract DE-AC02-80ER10722). G.B.E. thanks the Alfred P. Sloan Foundation for a Fellowship.

Registry No. $\text{CH}_2=\text{C}=\text{CH}^-$, 64066-06-4; $\text{CD}_2=\text{C}=\text{CH}^-$, 85048-63-1; $\text{CH}_2=\text{C}=\text{CD}^-$, 85048-64-2; $\text{HC}\equiv\text{CCH}_2^-$, 2932-78-7; $\text{HC}\equiv\text{CCD}_2^-$, 15650-79-0; $\text{DC}\equiv\text{CCH}_2^-$, 85048-65-3; CH_3CCH^- , 74-99-7; $\text{CH}_2=\text{C}=\text{CH}_2$, 463-49-0; $\text{CH}_3\text{C}\equiv\text{CH}$, 7299-37-8; $\text{CD}_3\text{C}\equiv\text{CH}$, 13025-73-5; $\text{CH}_3\text{C}\equiv\text{C}^-$, 36147-87-2.

Dynamic and Structural Properties of Polymerized Phosphatidylcholine Vesicle Membranes

Akihiro Kusumi,^{1a} Maninder Singh,^{1b} David A. Tirrell,^{1c} Gunther Oehme,^{1b} Alok Singh,^{1b} N. K. P. Samuel,^{1b} James S. Hyde,^{1a} and Steven L. Regen*^{1b}

Contribution from the Department of Chemistry, Marquette University, Milwaukee, Wisconsin 53233, the National Biomedical ESR Center, Department of Radiology, Medical College of Wisconsin, Milwaukee, Wisconsin 53226, and the Department of Chemistry, Carnegie-Mellon University, Pittsburgh, Pennsylvania 15213. Received September 7, 1982

Abstract: The phase transition, fluidity, and polarity properties of polymerized and nonpolymerized vesicle membranes derived from 1-palmitoyl-2-[12(methacryloyloxy)dodecanoyl]-L- α -phosphatidylcholine (**1**), bis[12-(methacryloyloxy)dodecanoyl]-L- α -phosphatidylcholine (**2**), and 1,2-dipalmitoyl[N-2-(methacryloyloxy)ethyl]-DL- α -phosphatidylcholine (**3**) have been examined by means of differential scanning calorimetry and by the spin-labeling technique. Above 5 °C aqueous multilamellar dispersions of **1**, **2**, and **3** show a broad-phase transition, no phase change, and a sharp transition, respectively. Polymerization of the methacrylate group causes a decrease in membrane fluidity in each case and an increase in the temperature of the gross phase change for **1** and **3**. Membrane fluidity in copolymerized vesicles of **1** and **2** decreases linearly with the mole fraction of **2** used. The polarity gradient in membranes of **3** is small; polarity gradients in membranes of **1** and **2** are large. Polymerization has no noticeable effect on these gradients. Fluidity gradients are also present in membranes of **1**, **2**, and **3** above 20 °C. Polymerization alters the fluidity gradients in a manner which is comparable to lowering the temperature; it also reduces the ability of each membrane to bind [¹⁵N]perdeuteriotempon. These results are compared directly with the dynamic and structural properties found in conventional liposomes derived from dipalmitoylphosphatidylcholine and egg yolk phosphatidylcholine.

Polymerized forms of lipid bilayer vesicles have recently been described by several laboratories.²⁻⁹ Because of their enhanced stability, this unique class of polymers offers an attractive alternative to conventional liposomes as models for biological membranes, devices for solar energy conversion, and carriers of drugs.¹⁰⁻¹⁸ While considerable interest has centered around their synthetic design, polymerization behavior, gross morphology, entrapment efficiency, permeability, and stability, relatively little attention has focused on the dynamic and structural features of the membrane network.

In this paper we report the results of a spin-labeling study and a differential scanning calorimetry (DSC) analysis aimed at characterizing the phase transition, fluidity, and polarity properties of polymerized and nonpolymerized vesicle membranes derived from 1-palmitoyl-2-[12-(methacryloyloxy)dodecanoyl]-L- α -phosphatidylcholine (**1**), bis[12-(methacryloyloxy)dodecanoyl]-

L- α -phosphatidylcholine (**2**), and 1,2-dipalmitoyl[N-2-(methacryloyloxy)ethyl]-DL- α -phosphatidylcholine (**3**). Our reasons

(1) (a) National Biomedical ESR Center. (b) Marquette University. (c) Carnegie-Mellon University.

(2) Regen, S. L.; Czech, B.; Singh, A. *J. Am. Chem. Soc.* **1980**, *102*, 6638. Regen, S. L.; Singh, A.; Oehme, G.; Singh, M. *Biochem. Biophys. Res. Commun.* **1981**, *101*, 131. Regen, S. L.; Singh, A.; Oehme, G.; Singh, M. *J. Am. Chem. Soc.* **1982**, *104*, 791.

(3) Hub, H. H.; Hupfer, B.; Koch, H.; Ringsdorf, H. *Angew. Chem., Int. Ed. Engl.* **1980**, *19*, 938.

(4) Akimoto, A.; Dorn, K.; Gross, L.; Ringsdorf, H.; Schupp, H. *Angew. Chem., Int. Ed. Engl.* **1981**, *20*, 90.

(5) Johnston, D. S.; Sanghera, S.; Pons, M.; Chapman, D. *Biochim. Biophys. Acta* **1980**, *602*, 57.

(6) Lopez, E.; O'Brien, D. F.; Whitesides, T. H. *J. Am. Chem. Soc.* **1982**, *104*, 305. O'Brien, D. F.; Whitesides, T. H.; Klingbiel, R. T. *J. Polym. Sci., Polym. Lett. Ed.* **1981**, *19*, 94.

(7) Gros, L.; Ringsdorf, H.; Schupp, H. *Angew. Chem., Int. Ed. Engl.* **1981**, *20*, 305. Folda, T.; Gros, L.; Ringsdorf, M. *Makromol. Chem. Rapid Commun.* **1982**, *3*, 167.

* Alfred P. Sloan Fellow, 1982-1984.

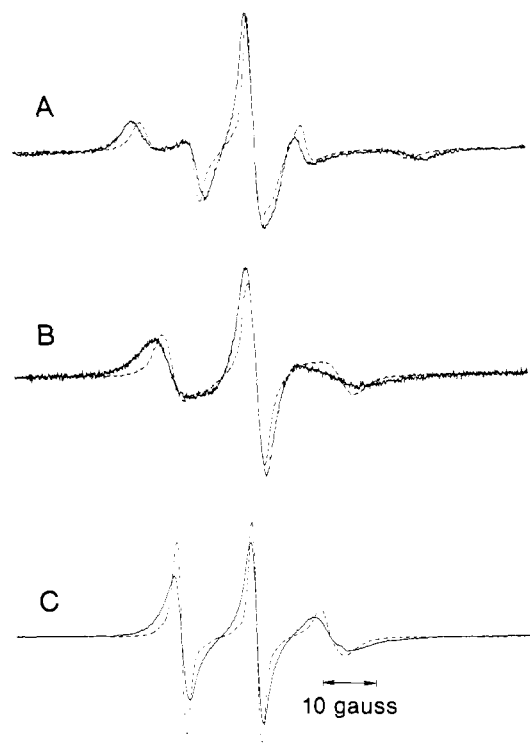


Figure 2. Representative esr spectra of (A) 5-SASL in membranes of 2, (B) ASL in membranes of 1, and (C) 16-SASL in membranes of 1 before (broken line) and after (solid line) polymerization at 30 °C.

of compound 3 was unchanged on subsequent heatings and was insensitive to variations in the heating rate from 10 to 16°/h.

Nitroxide Free Radicals as Molecular Probes for Mobility and Polarity. The electron spin resonance (ESR) spectrum of nitroxide free radicals located within liposomal membranes provides insight into the dynamic and structural properties of the membrane.^{27,28} In this study we have used a homologous series of spin probes for examining fluidity and polarity at different distances (depths) from the vesicle surface. Specifically, stearic acid derivatives having the 2,2-dimethyl-*N*-oxylazolidine (doxyl) ring at selected positions (i.e., 5-, 7-, 12-, and 16-SASL; Figure 1) were employed.^{28,29} In order to further characterize the phase behavior of membranes made of 1, 3-doxyl-5 α -androstan-17 β -ol (ASL), a steroid analogue, was also used. In contrast to the stearic acid labels, the steroidal nitroxide has a rigid structure and its mobility, as reflected by its ESR spectrum, relates to the motion of the molecule as a whole rather than the segmental flexibility of the alkyl chains.

Fluidity within Nonpolymerized Vesicle Membranes. Representative ESR spectra of 5-SASL, 16-SASL, and ASL incorporated into polymerized and nonpolymerized membranes are shown in Figure 2. Distinct changes in the overall line shapes are clearly observed after polymerization. The distance between the outer extrema (i.e., the maximum splitting) reflects the degree of order of the alkyl chains around the spin label.^{27c} As the mobility decreases the maximum splitting increases. Since the location of fatty acid spin labels in vesicle membranes is better defined when they are in their unprotonated form,³⁰ basic conditions were

used in all experiments (pH 7.0~9.5; see Experimental Section for details).

Figure 3 shows the maximum splitting observed for 5-SASL in membranes derived from monomers 1, 2, and 3 as a function of temperature. For 3, a well-defined phase change is indicated at ca. 32 °C (Figure 3A). Since phase transition temperatures depend somewhat on their method of detection (and sample history), we regard this value as being in reasonably good agreement with the T_m value indicated by DSC.³¹ In contrast, the temperature dependence of the maximum splitting of 5-SASL in membranes of 1 reveals a very broad transition below 13 °C (Figure 3B) which also agrees with the above DSC results. Reporter molecules 16-SASL and especially ASL confirm the presence of a broad transition in this temperature region (parts C and D of Figure 3). As expected from the DSC data the maximum splitting of 5-SASL in membranes of 2 changes continuously with temperature and does not show any indication of an abrupt phase change above 0 °C (Figure 3B).

Fluidity within Polymerized Vesicle Membranes. Figure 3 further shows how polymerization influences the fluidity within membranes of 1–3. For 3, the transition temperature is shifted to ca. 37 °C (5° increase) and is slightly broadened. Polymerization of 1 also decreases membrane fluidity at each temperature and shifts the broad transition to a higher temperature range (Figure 3C). Finally, polymerized phospholipid dispersions of 2, which are capable of forming cross-linked membrane networks, show no evidence of a phase change from 0 to 50 °C. All of these results are fully consistent with the DSC data described in the previous section. It is also interesting to note that between 5 and 50 °C polymerization with cross-linking is approximately two times as effective in reducing membrane fluidity as is polymerization without cross-linking (Figure 3B). Data presented in Figure 4 also show that the fluidity within membranes formed by copolymerization of 1 and 2 decreases in proportion to the mole fraction of 2. These results indicate that fluidity can be “fine-tuned” by varying the cross-link density.

Polarity and Flexibility Gradients. Griffith et al. have shown that the maximum splitting observed for spin labels under conditions where rotational motion is frozen reflects the polarity surrounding the nitroxide moiety.²⁹ The maximum splitting for 5-, 7-, 12- and 16-SASL in DPPC and in egg yolk phosphatidylcholine vesicles at -100 °C is plotted in Figure 5A. The observed values were unchanged by lowering the temperature to -150 °C. A large polarity gradient is clearly visible within the egg yolk phosphatidylcholine; with DPPC, however, the gradient is much less pronounced. Releasing the labels from the frozen state by increasing the temperature resulted in the formation of well-defined flexibility gradients in the ESR spin label time scale for both membranes (Figure 5A).²⁸

The maximum splitting observed for this same series of stearic acid spin labels in membranes of 3 at several temperatures (before and after polymerization) are shown in Figure 5B. At -100 °C, a very small polarity gradient is observed similar to that found for DPPC; polymerization has no noticeable effect on this gradient. Above 20 °C, flexibility gradients are observed for both polymerized and nonpolymerized vesicles; the mobility of each of the labels is, however, lower in the polymerized sample at all temperatures.

In contrast to 3, significant polarity gradients are observed within the polymerized and nonpolymerized membranes of 1 and 2 and are similar to that found for egg yolk phosphatidylcholine (parts C and D of Figure 5); polymerization produces no significant effect on these gradients. Flexibility gradients at temperatures greater than 20 °C are also substantial. Moreover,

(27) (a) Schreier, S.; Polnaszek, C. F.; Smith, I. C. P. *Biochim. Biophys. Acta* **1978**, *515*, 395. (b) Griffith, O. H.; Jost, P. C. In “Spin Labeling: Theory and Applications”; Berliner, L. J., ed.; Academic Press: New York, 1976; Chapter 12. (c) Marsh, D.; Watts, A. In “Liposomes: from Physical Structure to Therapeutic Applications”; Dingle, J. T., Gordon, J. L., Eds.; Elsevier: New York, 1981; Vol. 7, p 139.

(28) McConnell, H. M. In “Spin Labeling: Theory and Applications”; Berliner, L. J., Ed.; Academic Press: New York, 1976; Chapter 13. McConnell, H. M.; McFarland, B. G. *Ann. N. Y. Acad. Sci.* **1972**, *195*, 207.

(29) Griffith, O. H.; Behlinger, P. J.; Van, S. P. *J. Membr. Biol.* **1974**, *15*, 159.

(30) (a) Sanson, A.; Ptak, M.; Rigand, J. L.; Gary-Bobo, C. M. *Chem. Phys. Lipids* **1976**, *17*, 435. (b) Kusumi, A.; Subczynski, W. K.; Hyde, J. S. *Fed. Proc., Fed. Am. Soc. Exp.* **1982**, *41*, 1394 (Abstract 6571).

(31) For another example in which the ESR phase transition temperature was lower than that indicated by DSC, see ref 27c, p 145. It should be noted that 5-SASL does not show any discontinuity in the maximum splitting at the main phase transition of DPPC, which is reflected as an inflection in the plot of parts A and B of Figure 3 at 40–41 °C. The observed ESR line shape does, however, change dramatically at the main phase transition. The large change in the maximum splitting of 5-SASL in DPPC corresponds to a pretransition (see ref 30b for details).

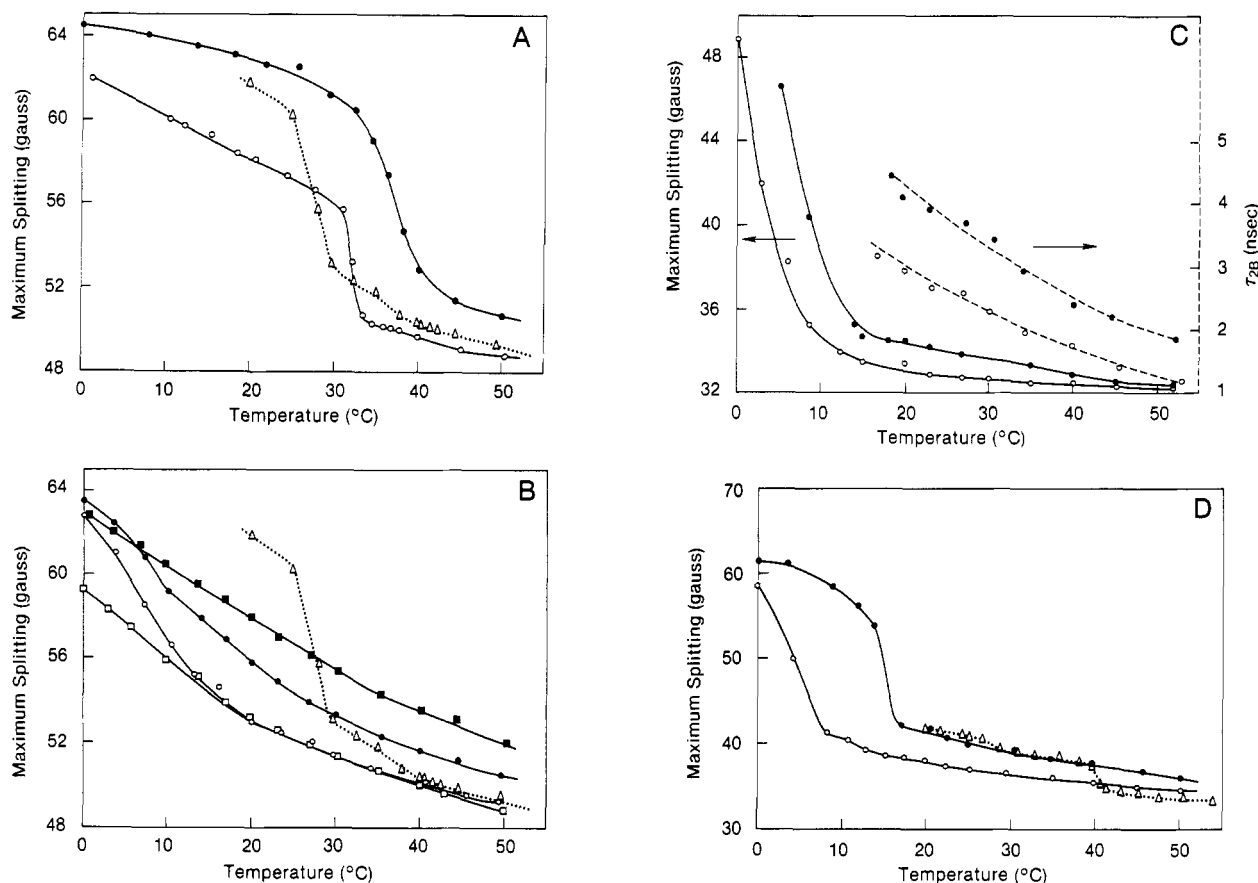


Figure 3. A. Maximum splitting value of 5-SASL in membranes made from 3 plotted against temperature before (○) and after (●) polymerization. DPPC data (△) are also shown for comparison. The main phase transition of DPPC is reflected by an inflection at ca. 40 °C; the pretransition appears as a sharp change in the maximum splitting at ca. 28 °C. B. Maximum splitting value of 5-SASL in membranes made from 1 (○, ●) and 2 (□, ■) before (open marks) and after (closed marks) polymerization plotted against temperature. DPPC data (△) are also shown for comparison. C. Maximum splitting value (solid line, left) and rotational correlation time (broken line, right) of 16-SASL in 1 plotted against temperature before (○) and after (●) polymerization. Rotational correlation times were calculated according to $T_{2B} = (6.51 \times 10^{-10}) \cdot \Delta H_0 [(h_0/h_{-1})^{1/2} - (h_0/h_{+1})^{1/2}]$, where ΔH_0 denotes the peak-to-peak line width in gauss and h_{+1} , h_0 , and h_{-1} represent the peak heights of the low-, central-, and high-field absorption lines: Stone, T. J.; Buckman, T.; Nordio, P. L.; McConnell, H. M. *Proc. Natl. Acad. Sci. U.S.A.* **1965**, *54*, 1010. D. Maximum splitting value of ASL in 1 plotted against temperature before (○) and after (●) polymerization. DPPC data (△) are also shown for comparison.

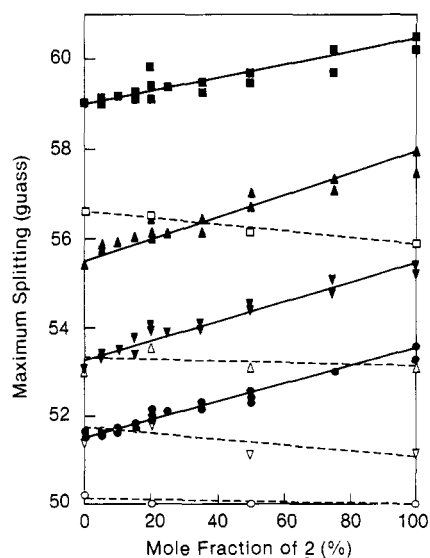


Figure 4. Maximum splitting value of 5-SASL in membranes made from mixtures of 1 and 2 as a function of mole fraction of 2 before (open marks) and after (closed marks) polymerization; 10 °C (□, ■), 20 °C (△, ▲), 30 °C (▽, ▼), and 40 °C (○, ●).

polymerization reduces the mobility of the labels and alters the fluidity gradient in a manner which is comparable to lowering the temperature (compare the fluidity profile for nonpolymerized 1 at 20 °C with polymerized 1 at 40 °C; also, compare non-

polymerized 2 at 20 °C with polymerized 2 at 40 °C).

Partitioning of Tempone into Polymerized and Nonpolymerized Vesicle Membranes. In order to determine the influence that polymerization has on the binding properties of vesicle membranes, the partitioning of [^{15}N]perdeuteriotempone between hydrophilic and hydrophobic regions of multilamellar dispersions of 1, 2, and 3 was examined. This specific spin label was chosen because it has reasonable solubility in both organic and aqueous phases and because the high field absorption can be clearly resolved into aqueous and membrane-bound components.³² In this study we have also used the perdeuterated form of the label since it allows for greater spectral resolution. The peak-height ratio h_m/h_w (where h_m is the height of the membrane component and h_w is the height of the aqueous component) of the high-field absorptions of tempone reflects the partitioning of the label. As can be seen in Figure 6, polymerization restricts the partitioning of the probe into each of the membranes. Moreover, polymerization substantially reduces the temperature dependence of the partitioning. The lesser ability of polymerized vesicle membranes to bind substrates is undoubtedly responsible for their reduced permeability.²

Conclusions

The phase transition, fluidity, polarity, and binding properties of polymerized and nonpolymerized vesicle membranes derived from 1, 2, and 3 have been examined by means of differential scanning calorimetry and by the spin-labeling technique. Principal conclusions that emerge from this study are the following: (1)

(32) See ref 27a, p 416.

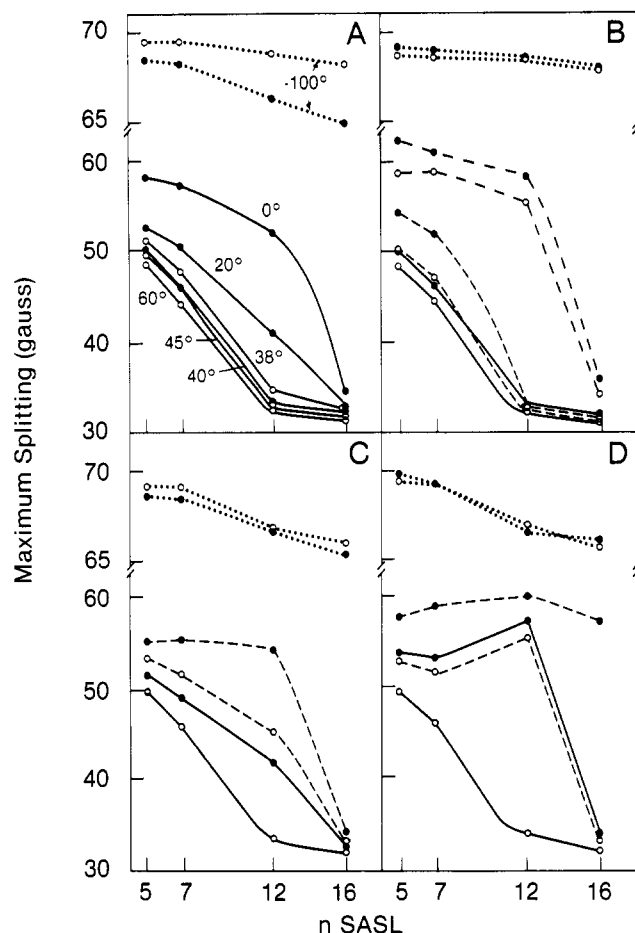


Figure 5. Maximum splitting values of stearic acid spin labels plotted against the attachment site of the doxyl ring. A: DPPC (○) and egg yolk phosphatidylcholine (●). B: **3** before (○) and after (●) polymerization at -100°C (dotted line), 20°C (broken line, upper two curves), 40°C (broken line, lower two curves), and 60°C (solid line). C: **1** before (○) and after (●) polymerization at -100°C (dotted line), 20°C (broken line), and 40°C (solid line). D: **2** before (○) and after (●) polymerization at -100°C , 20°C (broken line), and 40°C (solid line).

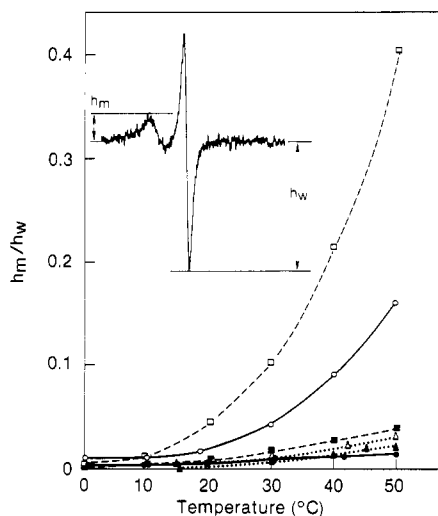


Figure 6. The peak-height ratio (h_m/h_w) for $[^{15}\text{N}]$ perdeuteriotempone partitioned between hydrophilic and hydrophobic regions in multilamellar dispersions of **1** (□, ■), **2** (○, ●), and **3** (△, ▲) before (open marks) and after (closed marks) polymerization. The spectrum included in the figure shows the typical resolution observed for the high field absorptions.

The incorporation of a methacrylate group either in the head group or the terminus of the β chain of a phosphatidylcholine molecule results in a lowering and broadening of the main phase transition relative to DPPC dispersions; attachment to both α and β chains

eliminates entirely the "main transition" above 5°C . (2) Polymerization of the methacrylate groups causes a decrease in membrane fluidity and an increase in the temperature of the gross phase change. (3) Polymerization with cross-linking has approximately twice as large an effect (between 5 and 50°C) in reducing the mobility of membrane-bound 5-SASL than does polymerization without cross-linking. (4) Membrane fluidity in copolymerized vesicles of **1** and **2** decreases linearly with the mole fraction of **2** employed. (5) The polarity gradient in membranes of **3** is small and similar to that found for DPPC; polarity gradients in **1** and **2** are large and similar to that observed in egg yolk phosphatidylcholine; polymerization has no noticeable effect on these gradients. (6) Fluidity gradients are present in membranes of **1**, **2**, and **3** above 20°C ; polymerization reduces the mobility of the labels and alters the fluidity gradients in a manner which is comparable to lowering the temperature. (7) Polymerization of the membranes of **1**, **2**, and **3** reduces their ability to bind $[^{15}\text{N}]$ perdeuteriotempone.

In summary, polymerized phosphatidylcholine vesicle membranes, "stitched together" at the head group or at the hydrocarbon core via methacrylate groups, retain the basic elements which characterize the dynamic and structural properties found in conventional liposomes. They exhibit phase transition behavior and fluidity and polarity gradients which are similar to those of nonpolymerized analogues.

Experimental Section

General Methods. Unless stated otherwise, all reagents and chemicals were obtained commercially and used without further purification. L- α -Dipalmitoylphosphatidylcholine was purchased from Sigma (St. Louis, MO). All stearic acid derived and androstane-derived spin labels were purchased from Molecular Probes (Plano, TX). $[^{15}\text{N}]$ perdeuteriotempone was obtained from Merck (Montreal, Canada). Lipids **1** and **2** were synthesized as described previously.²

Differential Scanning Calorimetry. Calorimetric scans were taken on a Microcal MC-1 scanning calorimeter, at heating rates of 10 – $22^{\circ}\text{C}/\text{h}$. Multilamellar dispersions containing 2.0 mg/mL of lipid were prepared by hydration of dried lipid films with 0.2 M sodium phosphate buffer, pH 7.4 – 7.7 , under vigorous agitation on a vortex mixer at 50°C . These dispersions were used directly for calorimetry, either before polymerization or after polymerization according to the procedure described previously.²

Sample Preparation and ESR Measurements. The membranes used in this work were multilamellar dispersions of lipids prepared in the following way. Lipid ($1.0 \times 10^{-5}\text{ mol}$) in chloroform was dried with a stream of nitrogen and further dried under a reduced pressure (0.1 mmHg). One milliliter of aqueous buffer was added to the dried lipid, and the dispersion was then vortexed vigorously at 50°C . Buffer solutions used in this work were 0.2 M sodium phosphate at pH 7.8 for 5-SASL and at pH 7.0 for ASL and tempone, a 0.1 M sodium borate buffer at pH 9.5 was used for 16-SASL. The membranes were polymerized in a UV chamber (254 nm) for 1 h .² In all cases, the extent of polymerization was quantitative as judged by TLC (polymerized lipids do not move from the origin on silica gel using $65:25:4\text{ CHCl}_3\text{-CH}_3\text{OH-H}_2\text{O}$). For the spin labeling of the membranes, a thin film of the desired spin label was coated onto the bottom of a test tube by solvent evaporation and the multilamellar dispersion of lipids (polymerized or nonpolymerized) was then added and incubated at 50°C for 30 min . The mole ratio of spin label to lipid was $1:200$, but the signal intensity was much weaker than that of the sample that was prepared by mixing lipid and spin label at the same ratio in chloroform solution (without polymerization). This indicates that the incorporation efficiency of lipid spin labels by the incubation method is low; about 5 – 10% of the label became incorporated. The ESR spectrum was the same for samples spin labeled by both methods and showed no dependence on the concentration of the label. The use of the incubation method proved necessary, however, because of the photolability of the spin labels at 254 nm .³³ The lipid dispersion was centrifuged briefly, and the loose pellet was used for ESR measurements. For tempone partition experiments, a 10 mM lipid dispersion was mixed with a tempone solution (0.5 mM final concentration) and incubated at 50°C for 30 min . The sample was then centrifuged at 4°C for 5 min . The samples were taken in a capillary (0.9-mm i.d.) made of gas permeable methylpentene polymer known as TPX.³⁴ This plastic is permeable to nitrogen, oxygen, and carbon dioxide

(33) Keute, J. S.; Anderson, D. R.; Koch, T. H. *J. Am. Chem. Soc.* **1981**, *103*, 5434.

and is substantially impermeable to water. Samples were placed inside the Dewar and equilibrated with nitrogen gas that was used for temperature control. ESR spectra were obtained with a Varian E-109 X-band spectrometer with Varian temperature control accessories and Varian E-231 multipurpose cavity (rectangular TE₁₀₂ mode). The sample was thoroughly deoxygenated in order to obtain correct line shapes of ESR spectrum and to prevent possible oxidation of lipids.

Synthesis of Phospholipid 3. Dipalmitoyl glycerol and 3-phosphoric acid bromoethyl ester³⁵ (300 mg, 0.377 mmol) were mixed with 4 mL of (dimethylamino)ethyl methacrylate and stirred in an oil bath for 40

h at 50 °C. Upon cooling the solution to room temperature, 30 mL of acetone was added. A colorless precipitate was formed on standing at -10 °C for 4 h. This crude product (307 mg) was then chromatographed on silica gel using conditions similar to those previously described,² to give 192 mg (0.231 mmol) of **3** having the expected IR and NMR spectrum.² Anal. Calcd for **1**: N, 1.68; P, 3.72. Found: N, 1.71; P, 3.75.

Acknowledgment. This work was supported by PHS Grant No. CA 28891 awarded by the National Cancer Institute^{1b} and Grants RR-01008 and GM-22923 from the National Institutes of Health.^{1a}

Registry No. **1**, 79481-27-9; **2**, 79605-84-8; **3**, 85168-67-8; tempone, 2896-70-0.

(34) Popp, C. A.; Hyde, J. S. *J. Magn. Reson.* **1981**, *43*, 249.

(35) Eibl, H. *Chem. Phys. Lipids* **1980**, *26*, 239.

Low Non-Koopmans' Ion States of Unsaturated Hydrocarbons. Semiempirical PERTCI Calculations¹

Reinhard Schulz, Armin Schweig,* and Werner Zittlau

Contribution from the Fachbereich Physikalische Chemie, Universität Marburg, D-3550 Marburg, West Germany. Received October 4, 1982

Abstract: A theoretical approach to the question of low shake-up ionizations in the photoelectron spectra of unsaturated polyene-like hydrocarbons is made. PERTCI calculations including all singles and doubles with respect to the Koopmans' configurations as well as to the shake-up configurations were made using semiempirical MNDO, CNDO/S, and LNDO/S wave functions. The method was applied to butadiene, 1,1,4,4-tetrafluorobutadiene, *p*-xylylene, *o*-xylylene, isobenzofulvene, isobenzofulvenallene, 2,2-dimethylisoidene, and benzocyclobutadiene. Calculated ionization spectra for all of these systems are presented. They are compared with the UV photoelectron spectra of the molecules and, for 2,2-dimethylisoidene, with the UV/VIS spectrum of its cation. The results show that in all cases where photoelectron bands or shoulders of low intensity were ascribed to shake-up ionizations (e.g., tetrafluorobutadiene and *p*-xylylene) this was done for good reasons. The results further encompass new cases (e.g., isobenzofulvene, isobenzofulvenallene, and benzocyclobutadiene), for which low shake-up ionizations are predicted that cannot be observed in the photoelectron spectra due to their low intensities. These cases call for prompt measurements of the UV/VIS spectra of the corresponding cations.

Introduction

The interpretation of UV photoelectron (outer valence) spectra is usually based on the one-electron model of ionization, i.e., Koopmans' approximation, neglecting effects of electron correlation and reorganization. This is true for the overwhelming majority of *ab initio* as well as semiempirical calculations although it is known that Koopmans' approximation leads to wrong results for strongly localized molecular orbitals.² Two prominent examples of this failure are the ion state sequences of 1,4- and 1,2-benzoquinones.^{3,4} These can correctly be obtained only as n, n, π, π and n, π, n, π , respectively, if configuration interaction is admitted. In the inner valence region, the one-electron description is often effectively useless due to strong mixing between Koopmans' and non-Koopmans' configurations.⁵ As a consequence, numerous satellite bands emerge in the calculated photoelectron spectra. The interaction between Koopmans' and non-Koopmans' configurations can be so pronounced that a distinction between main bands and satellite bands is no longer possible. In addition, strong interaction between Koopmans configurations via non-Koopmans configura-

tions has recently been demonstrated.⁶

In accordance with these experiences all ion state calculations and thus interpretation of photoelectron spectra in our group have therefore been based on a large-scale configuration interaction treatment as a routine for many years, even in the low-energy (outer valence) region. Such a procedure guarantees that non-Koopmans' effects such as alterations in ion state sequences due to electron reorganization, correlation or Koopmans' state interactions via non-Koopmans' state interactions, and the appearance of low excited non-Koopmans' ion states (satellites or shake-up bands in the photoelectron spectra) are automatically taken into account.

Below we apply our configuration interaction approach in conjunction with semiempirical wave functions to unsaturated hydrocarbons, thus either confirming or predicting the existence of low shake-up ion states for these molecules.⁷ Transitions to such states may show up in the photoelectron spectra of these systems and/or the UV/VIS absorption spectra of the corresponding cations. The results clearly demonstrate the importance and the advantage of a many-electron approach to the prediction

(1) Part 99 of Theory and Application of Photoelectron Spectroscopy. For Part 98, see Schulz, R.; Schweig, A. *J. Electron Spectrosc. Relat. Phenom.* **1982**, *28*, 33.

(2) See, e.g., Lauer, G.; Schulte, K.-W.; Schweig, A. *Chem. Phys. Lett.* **1975**, *32*, 163, and references quoted therein.

(3) Lauer, G.; Schäfer, W.; Schweig, A. *Chem. Phys. Lett.* **1975**, *33*, 312.

(4) Eck, V.; Lauer, G.; Schweig, A.; Thiel, W.; Vermeer, H. *Z. Naturforsch.* **1978**, *33a*, 383.

(5) Cederbaum, L. S.; Domcke, W.; Schirmer, J.; von Niessen, W.; Dircksen, G. H. F.; Kraemer, W. P. *J. Chem. Phys.* **1978**, *69*, 1591.

(6) von Niessen, W.; Bieri, G.; Schirmer, J.; Cederbaum, L. S. *Chem. Phys.* **1982**, *65*, 157.

(7) Semiempirical SECI estimations of shake-up ionizations in the photoelectron spectra of polyene-like molecules were also made (a) by Koenig, T., personal communication, 1981, and Koenig, T.; Klopfenstein, C. E.; Southworth, S.; Hoobler, J. A.; Wilesek, R. A.; Balle, T.; Shell, W.; Imre, D. *J. Am. Chem. Soc.* **1983**, *105*, 2256, for *p*-xylylene, its dimethyl and perfluoro derivatives and tetrafluorobutadiene, and (b) by Kluge, G.; Scholz, M. *Int. J. Quant. Chem.* **1981**, *20*, 669, for butadiene.